Air Fluorescence Studies for Cosmic Ray Detection

M. M. Fraga[1], A.Onofre[1,2], N.F.Castro[1], F.Fraga[1], L. Pereira[1], F.Veloso[1], P.Vieira[1], S.Fetal[1,3], R. Ferreira Marques[1], M.Pimenta[4], A.Policarpo[1],

***Abstract*— The detection of fluorescence radiation produced in the atmosphere by an incoming ultra high energy cosmic ray, is a technique that has been used already by several experiments like Hires and Auger. A small fraction of the cosmic ray energy loss (~5 x 10^{-5}) appears as UV light, known as *air fluorescence*, and is emitted isotropically in the wavelength region between 300 and 420 nm. This emission results from the radiative de-excitation of the N_2 $C^3\Pi_u$ molecular state (2nd positive system). The dependence of the fluorescence light yield of N_2 is studied in this work as a function of pressure and temperature, using α-particles as excitation source.**

I. Introduction

THE detection of Ultra High Energy Cosmic Rays (UHECR) with energies above 10^{19}eV has become a very interesting and challenging problem of nowadays astrophysics. At this energy scale, the Greisen-Zatsepin-Kuzmin (GZK)[1] effect (known as the GZK-cutoff) should lead to a suppression of cosmic rays with energies above 5x10^{19}eV, if they are of extragalactic origin. The disagreement between the results from the AGASA [2] experiment (where events are observed above the GZK-cutoff) and the HiRes [3] experiment (where data is consistent with the existence of the GZK-cutoff) requires new high statistics experiments, like Auger [4], with improved detection capabilities for UHECR. When a cosmic ray enters the atmosphere it looses energy in the collisions along its path and produces an air-shower. A small fraction of the cosmic ray energy loss (~5 x 10^{-5}) appears as ultraviolet (UV) light, known as *air fluorescence*, that results from the radiative de-excitation of molecular nitrogen. This light is emitted isotropically in the wavelength region between 300 and 420 nm and consists of two systems of vibrational transitions: the second positive system (2P) of the N_2 molecule, (the $C^3\Pi_u$,v' → $B^3\Pi_g$,v" transitions) and the first negative system (1N) of the nitrogen ion, N_2^+, (the $B^2\Sigma_u^+ \rightarrow X^2\Sigma_g^+$ transitions) [5]. The intensity of the fluorescence light is a direct measure of the energy loss, from which the cosmic ray primary energy can be reconstructed. This technique is of utmost importance for the precise determination of the cosmic ray energy, and needs to be studied under very well controlled conditions at lab. In this work we study the fluorescence light yield from nitrogen, as a function of pressure and temperature, using α-particles from an ^{241}Am radioactive source.

[1] LIP- Coimbra, Dep. Física, Universidade de Coimbra, 3004-516 Coimbra, Portugal.
[2]UCP, R. Dr. Mendes Pinheiro, 24, 3080 Figueira da Foz, Portugal.
[3] ISEC, Quinta da Nora, 3030-199 Coimbra, Portugal.
[4] LIP-IST, Av. Elias Garcia 14, 1100-149 Lisboa, Portugal.

II. The Nitrogen Primary Scintillation

The structure of the light spectrum emitted by the molecular nitrogen can be studied using energetic α–particles as the excitation source. As the α-particle travels through gaseous nitrogen, at a given pressure and temperature, it looses energy along its path in ionization and excitation collisions. However, direct excitation of the N_2 $C^3\Pi_u$ molecular state by the α-particle is forbidden and no experimental evidence was found for its population by cascades from higher electronic molecular states. The only channel for the excitation of the N_2 $C^3\Pi_u$ state is thus, believed to be by collisions with the primary and secondary electrons produced in the gas by the α-particle. As the electron impact cross sections for the excitation of the N_2 $C^3\Pi_u$ vibrational levels (v'=0,1,2) peak at low energies, as shown in Fig.1, the secondary electrons produced in the cascade process initiated by the energetic primary particle, play a more important role in the N_2 fluorescence light yield (FLY) than the primary particle itself. As a consequence, the type of primary particle should not affect much the FLY unless collisional effects become important.

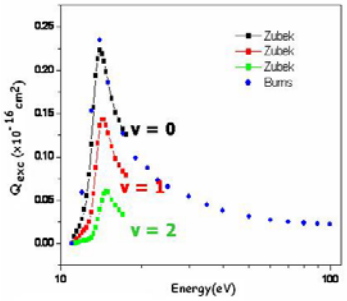

Fig.1 Excitation cross section of the vibrational levels v'=0, 1,2 of the N_2 $C^3\Pi_u$ electronic state by e- impact: squares correspond to the data of Zubek [7] and the circles correspond to the data of Burns [8].

The 2nd positive system of N_2 consists of a series of bands corresponding to the different $C^3\Pi_u$,v' → $B^3\Pi_g$,v'' vibrational transitions (with v'= 0,1,2,… and v''=0,1,2,..). The rotational structure of each band reflects the population distribution among the different rotational

levels of the upper state and the line strengths for each allowed transition. The band profiles were estimated [6] for different gas temperatures and for a very low gas pressure, where collisional effects are negligible. The histogram obtained with a bin of 0.1 nm, at room temperature, is shown in Fig. 2. The relative intensities of the different bands were obtained from the Einstein coefficients ($A_{v'v''}$), defined as the total transition probability from the molecular vibrational state v' to v''.

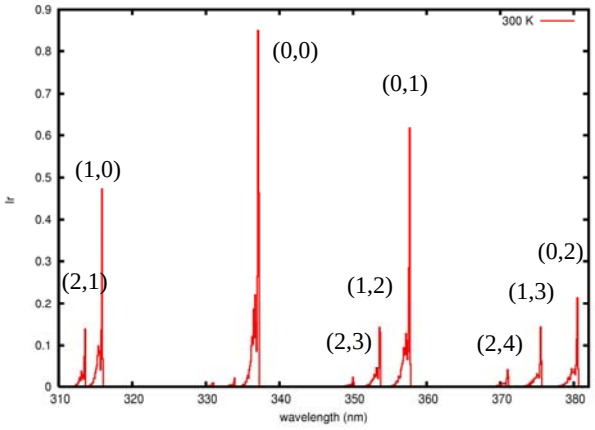

Fig. 2 – Band profiles for the 2P system of N_2 between 310 and 382 nm, for T = 300 K. Vibrational transitions (v',v'') are indicated on the spectrum

In steady state conditions the light yield for the $v' \rightarrow v''$ transition (in terms of number of photons per unit energy deposited) can be expressed by

$$Y_{v'v''} = A_{v'v''} [N_2^*] \tau_{v'}, \quad (1)$$

where $[N_2^*]$ is the excitation yield (the number of excited molecules per deposited energy) and $\tau_{v'}$ is the total de-excitation lifetime for the v´ state. The total lifetime for the v´ state is affected by the radiative decay time $\tau_{0v'}$ (where photons are actually emitted) and the collisional decay time $\tau_{cv'}$ (where de-excitation through collisions with gas molecules is accounted for) i.e.,

$$\frac{1}{\tau_{v'}} = \frac{1}{\tau_{0v'}} + \frac{1}{\tau_{cv'}} \ . \quad (2)$$

While the radiative component can be expressed as

$$\frac{1}{\tau_{0v'}} = \sum_{v''} A_{v'v''} = A_{v'} , \quad (3)$$

the collisional rate is given by

$$\frac{1}{\tau_{cv'}} = [N_2] \, \sigma \, v_r \, . \quad (4)$$

In Eq.(4), $[N_2]$ corresponds to the gas density (in number of particles per unit volume), σ is the de-activation collisional cross section and

$$v_r = \sqrt{\frac{8kT}{\mu\pi}} \quad (5)$$

corresponds to the mean velocity of the molecules in the gas (following a Maxwell-Boltzmann distribution for a given temperature T). As most of the measurements in this paper are performed at constant gas density, the total de-excitation time can be expressed as a function of temperature (assuming no dependence of σ with external factors like pressure, temperature or contributions from other gases) according to

$$\frac{1}{\tau_{v'}} = A_{v'} + B\sqrt{T} \ . \quad (6)$$

The constant B can be easily expressed in terms of the constants appearing in Eqs.(4) and (5). The total number of detected photons, N_{ph}, is proportional to the total fluorescence light yield (Eq.1). The constant of proportionality includes the filter and windows transmission, the quantum efficiency of the photomultiplier and a geometrical factor for the light collection. In the present experimental conditions this constant depends on the temperature. When all these factors are taken into account the corrected counting rate is expected to follow a temperature dependence given by

$$R \propto (A_{v'} + B\sqrt{T})^{-1} \, . \quad (7)$$

Depending on the relative importance of $A_{v'}$ and B, a more or less significant increase of R is expected as the temperature goes down, for a given gas density.

III. Experimental Setup

The experimental setup used to study the FLY, as a function of temperature and pressure, is represented in Fig.3. It is composed of a stainless steel chamber (with diameter ϕ=50mm and width h=30mm) coupled to two XP2020Q photomultipliers (PM1 and PM2) through quartz windows. These PM´s are used to collect the nitrogen fluorescence. A Melles-Griot interference filter (with center wavelength λ_c=340nm, $\Delta\lambda$=10nm and peak transmission of 31%) is placed between the chamber and PM2 to isolate the 0-0 band (peaking at 337.1 nm). A vacuum pump is used to evacuate the chamber prior each gas filling. At the top of the chamber a 127 μm mylar window allows the α-particles from a non-collimated ^{241}Am source to get inside the chamber (Fig. 3). A pressure sensor (SETRA 216) and two temperature probes (PT100 with stabilized current source) are used to control and measure the pressure and temperature inside and outside the chamber. The chamber is inserted in a cooling unit which allows the temperature to change from room temperature down to -25ºC. In order to reduce the photomultipliers temperature gradient, PM1 and PM2 are housed in cylindrical PVC tubes (covered with black foam) which isolate them from the inside of the cooling unit.

The PM signals are amplified and shaped before being fed into a coincidence unit. The coincidence counting rate is recorded with the data acquisition system, FluDaq. This program is based on LabView and it also allows the remote

control of the temperature inside the cooling unit and the readout of the pressure sensor and temperature probes during each temperature cycle.

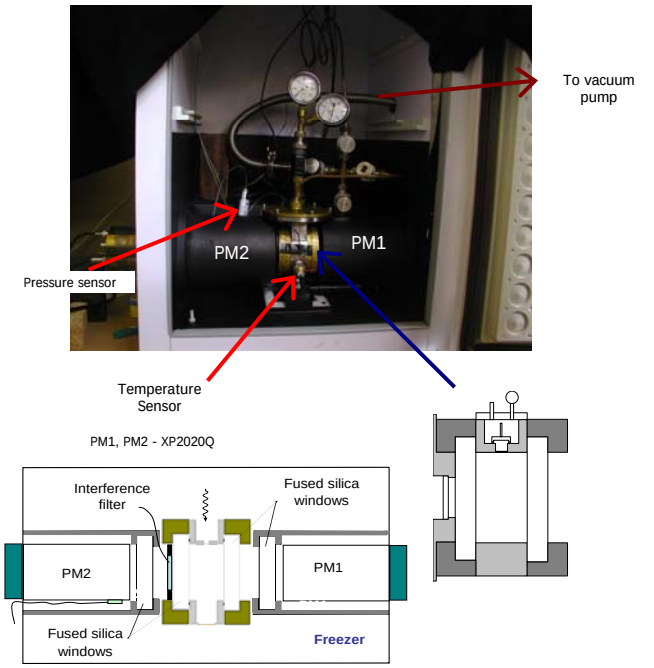

Fig. 3 – Experimental set-up used to study the FLY as a function of pressure and temperature using α particles as excitation source.

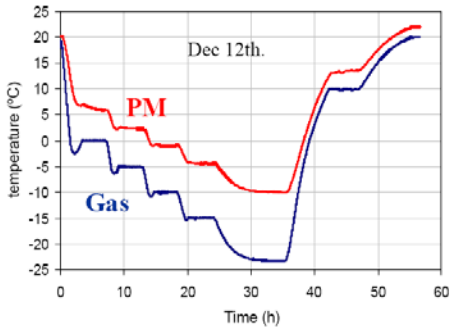

Fig.4 Typical cycle of temperature of the photomultiplier (PM) and the chamber (Gas) as a function of time.

A typical measurement cycle starts by evacuating the chamber for several hours, filling it afterwards with N_2 at a given pressure (and room temperature), closing the chamber and starting the temperature decrease by switching ON the cooling unit (Fig.4). During this process specific values of the chamber temperature are kept for longer periods of time in order to collect more statistics at these temperatures.

The variation of the coincidence counting rate, corrected for accidental coincidences, with the temperature is shown in Fig. 5, for different gas densities. All values are normalized to T=273 K and the error bars include only the statistical error contribution. As one can see the counting rate decreases with decreasing temperature, and the variation is more important for higher filling pressures.

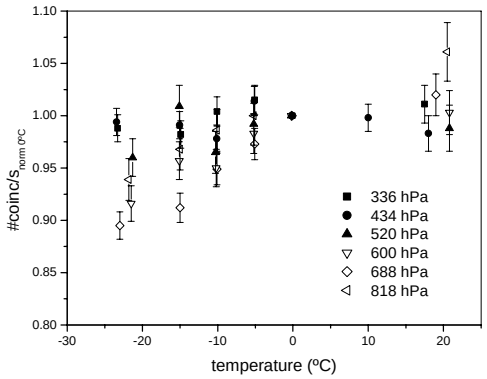

Fig. 5 – Number of coincidences, normalized at 0ºC, as a function of the temperature inside the chamber. The indicated values of the pressure refer to the pressure at room temperature.

IV. Monte Carlo Simulation

A GEANT4 [9] simulation of the set-up was developed in order to understand the dependence of the experimental data with pressure and temperature. The α particles are emitted from the source along a direction selected at random, cross a small layer of air outside the chamber and the mylar window, and get into the chamber. UV photons are emitted isotropically along the track. For this reason it is necessary to have a careful description of the different materials and optical interfaces the photons may encounter along their path.

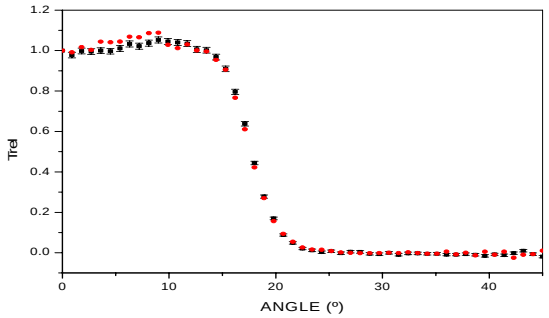

Fig. 6 – Interference filter response as a function of the positive (red) and negative (black) incidence angle (for λ=337nm).

One of the most important components of the optical system is precisely the interference filter placed in front of PM2. In Fig. 6, the transmission of the filter is represented as a function of the incidence angle (for λ=337.1nm).

In Fig.7 we represent an α-particle event simulation, for N_2 at a pressure of 336 hPa and 20ºC, with a 6 mm layer of air, at atmospheric pressure, between the α source and the mylar window.

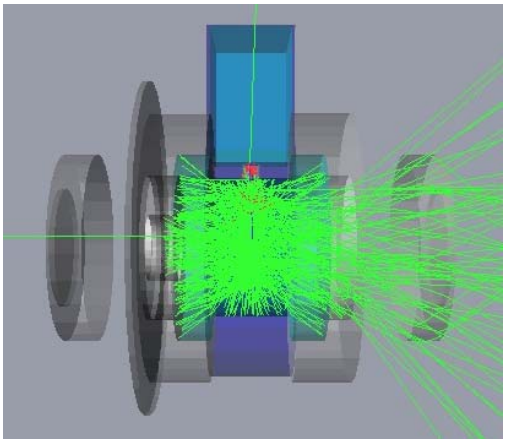

Fig.7 – Simulation of an α-particle event , with N_2 inside the chamber at a pressure of 336hPa and 20ºC, and air just before the mylar window.

The GEANT4 simulation of the chamber showed that two effects are important to understand the experimental behaviour of the data:

1. the transmission of the interference filter convoluted with the photon angular distribution produced by the α-particle along its path inside the chamber (which depends on the N_2 pressure);
2. the dependence of the length of the α-particle path inside the chamber with the temperature. As the α–particle crosses a layer of atmospheric air before entering the mylar window, whenever the temperature decreases, the air density increases increasing the α–particle energy loss outside the chamber.

These effects where accounted for in the GEANT4 simulation of the experimental set-up. For each pressure and temperature, correction factors were extracted from the simulation and used to correct the experimental data.

V. Results

The data represented in Fig. 5 were corrected for the factors discussed above, and the result is shown in Fig.8. Within the errors (only statistical), no variation with the temperature is observed. In order to test the performance of the GEANT4 simulation and the reliability of the correction factors, new data was acquired using α-particles and evacuating the region between the source and the mylar window. In this case, no correction factors associated to the energy loss of the α-particle in the air would be required. In Fig. 9 it is shown the relative number of photons emitted as a function of temperature for a pressure inside the chamber of 890 hPa, at room temperature. The two sets of data shown in the figure and represented by the red dots and blue triangles, correspond, respectively, to the decrease and increase temperature cycles of the chamber. Within the error bars, there is a good agreement between the results of Fig. 8 and Fig. 9.

The present simulation does not take into account the variation of transmission of the filter and the quantum efficiency of the photocathode of the photomultiplier with the temperature.

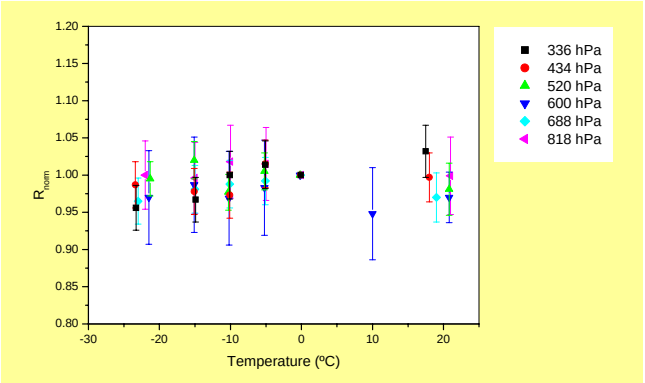

Fig.8 Relative number of coincidences between PM1 and PM2 as a function of the temperature inside the chamber after applying the correction factors (see text for details).

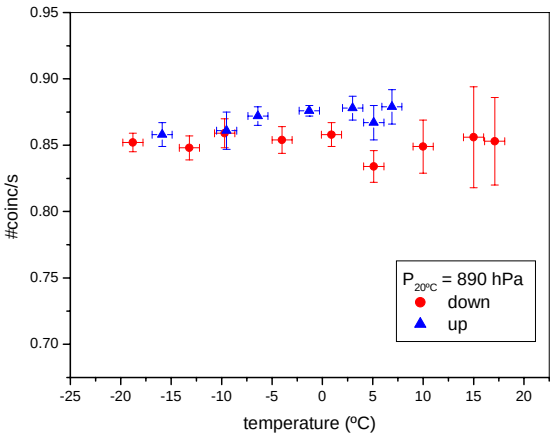

Fig.9 Relative number of coincidences between PM1 and PM2 as a function of the temperature inside the chamber with vacuum in front of the source.

VI. Conclusions

The detection of fluorescence radiation produced in the atmosphere by the incoming ultra high energy cosmic rays, is an important technique that has been used by the new generation experiments like Hires, Auger and, in the future, JEM-EUSO. This method is based on atmospheric nitrogen excitation by charged particles produced in the air shower, followed by the emission of photons in the range 300 nm – 420 nm. In the present work preliminary measurements of the fluorescence light yield of N_2 at 337.1 nm were performed as a function of temperature and pressure, using α–particles as excitation source. The apparent deviation from the expected theoretical behaviour of the light yield dependence with the temperature may be due to experimental effects that have not been introduced yet in

the simulation. Studies of the variation of the filter transmission and the sensitivity of the photomultiplier with the temperature are underway. In order to improve the precision of the measurements, a new chamber is under preparation which will allow the data acquisition with also electron sources.

ACKNOWLEDGMENT

This work was supported by the FCT under project POCTI/FP/63440/2005.

REFERENCES

[1] K.Greisen, *Phys. Rev.Lett*. 16 (1966) 748-750; G.Zatsepin ad V.Kuzmin, *JETP Lett.* 4 (1966) 78-80.
[2] K.Shinozaki and M.Teshima, (AGASA) *Nucl.Phys.Proc.Supp*. 136 (2004) 18-27.
[3] R.W.Springer (HiRes), *Nucl.Phys.Proc.Supp.* 138 (2005) 307-309.
[4] J.Abraham *et al.* (Auger), *Nucl.Inst.Meth*. A523 (2004) 50-95.
[5] R.W.B.Pearse and A.G.Gaydon, "*The Identification of Molecular Spectra*", Chapman and Hall Ltd, 11 New Fetter Lane, London EC4P 4EE, 1976.
[6] G. Hartmann and P. C. Johnson, *J. Phys. B* 11 (1978) 1597-1612.
[7] M. Zubek, J. Phys. B: At. Mol. Opt. Phys. 27 (1994) 573-581.
[8] D. J. Burns, F. R. Simpson, J W McConkey J. Phys. B: At. Mol. Phys. 2 (1969) 52-64.
[9] GEANT4—a simulation toolkit, *Nucl.Inst.Meth.* A 506 (2003) 250-303.